10-21-2005

Self-Assembly of Nanoparticles on Live Bacterium: An avenue to fabricate Electronic Devices

Vikas Berry
University of Nebraska-Lincoln, vberry2@unlnotes.unl.edu

Ravi F. Saraf
University of Nenraska-Lincoln, rsaraf2@unl.edu

Self-assembly of Nanoparticles on Live Bacterium via Teichoic Acid Brush: An Avenue to Fabricate Electronic Devices **

V. Berry & R. F. Saraf*

Department of Chemical Engineering, University of Nebraska – Lincoln, NE 68588, USA

rsaraf@unlnotes.unl.edu, Phone - 402-472-8284, Fax - 402-472-6989

** We thank Virginia Tech for accessibility to lab facilities during the early stages of this work. We thank Dr. Adenwalla at University of Nebraska – Lincoln for letting us use her low-temperature I-V measurement system.

Recently, hybrid structures of microorganisms with inorganic nanoscale moieties have received great interest due to their potential in fabricating electronic systems. Electronic properties of metal nanoparticles, due to single electron transport of current[1], make them ideal material for nanodevices. Concomitantly, the nanostructure of microorganisms such as bacteria[2], viruses[3;4] and yeast[5] are attractive scaffolds for nanoparticle templating due to surface charge and biological affinities for specific molecules [2-7]. However, the key challenges in building hybrid devices are patterning nanostructures without destroying the biological construct of the microorganism and achieving active integration of biological response to the electrical transport in nanoparticle device. Here we present a simple method to build hybrid devices that use biological response of the microorganism to control the electrical properties of the system. In our design, a monolayer of gold nanoparticles is deposited on the peptidoglycan membrane of a *live* gram-positive bacterium. The hydrophilic peptidoglycan membrane is then actuated by humidity, to modulate the electron tunnelling barrier width between the metallic

nanoparticles. A decrease in inter-particle separation by < 0.2 nm (for humidity excursion from 20% to ~0%) causes a > 40-fold increase in tunnelling current. Vapour sensors based on the increase in resistance due to separation of Au nanoparticles have been reported in three-dimensional (3D) clusters of Au nanoparticle/organic composite films[8-10]. In this study, the coupling between large expansion of an underlying hygroscopic bacterium membrane and the Au particle monolayer is the key to achieving an order of magnitude larger change in current compared to the above-mentioned 3D nanocomposite devices where the change is due to the swelling of an inter-particle organic phase. The method shown here could be used to pattern various nano-scale inorganics, whose optical, electrical and magnetic properties could be biologically controlled, bringing a prominent advancement in the present technology.

Electrically percolating clusters of metal nanoparticles, in contrast to their micro-particle cousins, are fundamentally different in terms of the electrical properties due to the nature of interparticle electron transport[1]. At nanoscale size, the charging energy to insert a single electron in nanoparticle is >1-10 fold the thermal energy, the inter-particle current flow is by single-electron transport as explicitly shown by transport studies on single-nanoparticle[11;12], their 2- and 3-dimesnsional assemblies[13-16], and single-nanoparticle devices (such as single-electron-transistor[17;18]). The above studies demonstrate that a percolating cluster of metal nanoparticles is a viable unit to fabricate single-electron devices, where the micron-scale clusters will allow for easy-to-fabricate, robust interconnection network for the nanodevice system. Because metal nanoparticles such as gold are stabilized in solution by electrostatic repulsion, forming a percolating cluster on physical substrates requires either an organic cross-linkers to stitch the particles[13;19] or polyelectrolyte to shield the charge of the particles[16;20]. For biological

substrates, the highly selective deposition of nanoparticles relies on either highly specific binding (such as DNA hybridization[21-23], biotin-streptavidin interaction[24]) or strong specific intermolecular interaction (such as electrostatic interaction[25-27]).

Bacillus cereus (a gram positive bacterium) is deposited on a poly-l-lysine (average molecular weight 164,000 Dalton) coated silicon substrate with 500 nm thermally grown silica and gold electrode lines at 7 ± 0.2 micron spacing, using a previously described technique[2]. In a typical deposition process, the bacteria are cultured in nutrient broth (Difco) in a shake flask for ~14 hrs. at 30 ^{O}C. The bacteria are subsequently filtered and centrifuged to extract similar sized cells that are ~ 4-6 μm long and ~ 0.8-1 μm in diameter. The bacteria are suspended again in sterile water and are deposited on the poly-l-lysine-coated substrate. On a substrate, there are 20 sets of electrodes. The deposition time of the bacteria is ~ 10-15 min. to form bridges spanning between the Au electrodes. Usually, ~10 bridges are formed along the 10 mm long Au electrode pair. The extra-cellular polymeric substances (EPS) on the bacteria (and around the bacterium) are removed by 2N NaOH wash for 1 min. The bacteria deposited chip is then immediately immersed in a solution of poly-l-lysine-coated gold nanoparticles (of diameter D=30 nm)[2]. Highly controlled deposition of nanoparticles is achieved by regulating the deposition time in the Au nanoparticle solution (see Fig. 1(a) to (e)). Since both the Au nanoparticles and the substrate are positively charged, the deposition is highly selective with a monolayer formation only on the (negatively charged) bacteria surface. However, a simple negative surface charge is not sufficient to obtain electrically percolating deposition. Fig. 1(f) shows deposition of the same Au nanoparticles on a negatively charged "physical surface" prepared by adsorbing monolayer of poly(sulfonated styrene)

(70,000 Daltons with <90% sulfonation) on the poly-l-lysine coated SiO_2/Si substrate (described above). Deposition was maximized by depositing poly-l-lysine and PSS at a pH of ~4 and ~8.5, respectively; and adding 1mM NaCl in the pH 7 suspension of the nanoparticle solution. However, the 2D packing density was found to be low and non-percolating. X-ray reflectivity measurements have shown that in the multi-layer films of polyelectrolytes (in our case PSS on poly-l-lysine) the polymers are layered and their conformations are flat with no significant loops due to multiple point binding[28].As a result, the polymer mobility is highly restricted. On the other hand, the polyelectrolyte on bacterium surface, i.e., the teichoic acid, is a flexible brush, tethered to the peptidoglycan surface at one end with rest of the chain in high thermal motion (i.e., high mobility). Furthermore, because the brush contour length is typically ~ 18 nm[29], it is reasonable to expect that the negatively charged teichoic acid molecule with high mobility and chain flexibility may wrap over the positively charged Au particle up to a maximum possible subtended angle of 135^{O} from the point of contact to minimize free-energy. A similar screening of charge by PSS would be difficult in the case for PSS/poly-l-lysine structure due to restricted mobility. Specific attachment of concanavalin-FITC dye to the teichoic acid[30] followed by confocal microscopy confirms their uniform distribution of the brush on the bacterium. Because, no nanoparticle deposition on the bacterium occurs subsequent to the neutralization of the teichoic acid after the attachment with concanavalin, the role of the latter in high-density deposition is justified.

A standard assay of PI/SYTO 9 dye is used to confirm the fate of the bacteria[31]. The green coloration in Fig. 3 shows that the bacteria survive the complete device fabrication process. Because integrity of the peptidoglycan surface membrane in which

the teichoic acid molecular-brush is imbedded is critical for the Au nanoparticle deposition, the survival of the bacteria for the device fabrication is important. Any lysis of the bacteria (or release of EPS and/or internal bacterial fluids) will lead to ill-formed, non-functional devices.

The inset of Fig. 4 shows a typical Au nanoparticle monolayer coated bacterial bridge connected to the Au electrodes. One bridge constitutes a device. All the currents reported subsequently are normalized by number of bridges between the electrodes and were measured at 22 ^{O}C. Fig. 4 shows the normalized current, I, between the bridges as a function of relative humidity R_H. The Au nanoparticle deposition is optimized for 4 hrs. (see Fig. 1(d)) to obtain the largest change in current due to humidity. Fig. 4 indicates that the device behaviour is reversible and stable over a slow run taken over ~40 min. per cycle. Because of complete reversibility of the device, it is unlikely that the water inside the bacteria plays any significant role. In contrast to most impedance based microelectronics humidity sensors[32], the resistance of the device decreases as humidity increases. The largest change in current,, and hence highest sensitivity, is for the low humidity region of R_H <20%.

A simple model based on Fig. 2 explains the observation in Fig. 4. As the humidity increases, the peptidoglycan membrane absorbs water. Assuming no excess volume of absorbed water, the volume fraction of water absorbed is fR_H, where f is Henry's constant. Assuming affine swelling of the peptidoglycan membrane, the linear extension of the membrane due to absorption is $(1-fR_H)^{-1/3}$. Because the nanoparticles are fixed on the membrane, the interparticle separation is given by, $a/a_O = (1-fR_H)^{-1/3}$, where a_O is the

separation at $R_H = 0$. Because electron tunneling is the primary transport mechanism, the current is given by Fowler-Nordheim equation [33],

$$I = \left\{ \frac{V}{R_0} \exp\left[-\frac{Ka_0}{\sqrt[3]{(1 - fR_H)}} \right] + \frac{V}{R_B} \right\} \quad (1)$$

where, $K = (32\pi^2 m_e \phi / h^2)^{0.5}$ (h is Plank's constant, m_e electron rest mass, and ϕ is the barrier height at nanoparticle/organic interface), R_B is the resistance to the leakage current from the peripheral as shown in Fig. 4, R_0 is a normalization constant proportional to device resistance at $R_H = 0$, and V is the bias across the device (i.e., bacteria bridge). We conjecture that the peripheral strip leading to finite R_B is due to deposition of proteinaceous substances secreted by the bacterium (probably for adhesion to the substrate). To decipher the effect of water absorption by poly-l-lysine on the device performance, after the device fabrication, we capped the amine groups of poly-l-lysine with glutaraldehyde to reduce the water uptake by lysine. No significant change in device performance was observed indicating that the role of moisture absorption by poly-l-lysine on device performance is negligible.

Fig. 5(a) shows the fit of the experimental observation to eq. (1) (for the same device) at different V. Each excursion in humidity was ~40 min. long and the lapse between consecutive runs on average was ~1 hr. Although eq. (1) has four fitting parameters, the validity of the model is justified because they are reasonably constant over all the biasing voltages (see Table in Fig. 5(a)). The constant R_B implies ohmic behaviour (independent of R_H) for leakage current given by, $I_B = V/R_B$. This is reasonable because on the peripheral region, the nanoparticles are not on the peptidoglycan membrane but adsorbed on to proteinaceous corona of the bacteria that does not change

significantly in the lateral dimension due to humidity. Because, the contact resistance is not expected to be large[2] and is a strong function of humidity, it is included in R_B. We also note that because the current through bacteria-bridge with no nanoparticles is insignificant, ionic currents can be neglected.

Fig. 5(b) shows the corrected current, $I - I_B$ that flows through the nanoparticle monolayer as a function of percent change in inter-particle separation (estimated from f). Interestingly, for a humidity change from 20 to 0% corresponding to calculated decrease in inter-particle distance of only 7%, the (corrected) current increase by over 40-fold. Because the corresponding increase in total current, I, is only ~7-fold (see Fig. 5(a)), a reduction in peripheral deposition will improve the device sensitivity significantly. The high sensitivity to subtle change in interparticle distance is attributed to transport by single-electron-tunneling through the percolation network because the charging energy $e^2/(2\pi\varepsilon\varepsilon_0 D) \sim 1.5kT$ (where, $\varepsilon \sim 3$ is the dielectric constant of the organic coating and e is electron charge). Using the model parameters, and a tunneling barrier of 5.1 eV (i.e., a is much larger than poly-l-lysine coating thickness in Fig. 2 implying metal(poly-l-lysine)/air/metal(poly-l-lysine) junction), the nanoparticle separation at 0% humidity is ~2.3 nm, implying an absolute change (for 0 to 20% humidity range) of <0.2 nm. We note that the sensitivity is significantly lower for devices fabricated at deposition time ≥ 8 hrs, where ohmic I-V is observed[2] than the non-ohmic behaviour for the reported 4 hrs. deposition time device (see inset of Fig. 5(b)). On the other extreme, for deposition time of 2 hrs. the inter-particle distance in the contiguous clusters is too large for significant tunneling current. Thus, a combination of exponential dependence on *a* and $a \sim 2.3$ nm explains the high sensitivity of the system. Furthermore, in contrast to the earlier reports

on Au/organic composite thin-film-sensors[8-10], where electron transport is by thermionic-emission or activated-tunneling, in our case, electron transport is via tunneling because the activation energy for tunneling is ~1.7 meV (see Fig. 6) which is much smaller than free-electron's thermal energy, kT ~ 25 meV at room temperature.

In summary, we have illustrated an approach to fabricate an active hybrid bio-electronic device using "physical" nanomaterials and a live microorganism. The electrical property of a monolayer of nanoparticles is controlled by actuating the peptidoglycan layer of the bacterium. A < 8% actuation in the peptidoglycan membrane, induced by humidity excursion from 20 to 0%, leads to > 40-fold increase in the tunnelling current. This work is a step forward in providing researchers an avenue to obtain active coupling between microorganisms and (electrical, optical and/or magnetic) physical nanodevices. We believe that such hybrids will be the key to conceptually new electronic devices that can be integrated with power and function of microorganisms, on flexible plastic-like substrates using simple beaker chemistry.

Reference List

[1.] B. Su, V. J. Goldman, J. E. Cunningham, *Science* **1992,** *255* 313-315.

[2.] V. Berry, S. Rangaswamy, R. F. Saraf, *Nano Letters* **2004,** *4* 939-942.

[3.] E. Dujardin, C. Peet, G. Stubbs, J. N. Culver, S. Mann, *Nano Letters* **2003,** *3* 413-417.

[4.] C. E. Fowler, W. Shenton, G. Stubbs, S. Mann, *Advanced Materials* **2001,** *13* 1266-1269.

[5.] M. Kowshik, S. Ashtaputre, S. Kharrazi, W. Vogel, J. Urban, S. K. Kulkarni, K. M. Paknikar, *Nanotechnology* **2003,** 95-100.

[6.] Z. Li, S. W. Chung, J. M. Nam, D. S. Ginger, C. A. Mirkin, *Angewandte Chemie-International Edition* **2003,** *42* 2306-2309.

[7.] N. L. Rosi, C. S. Thaxton, C. A. Mirkin, *Angewandte Chemie-International Edition* **2004,** *43* 5500-5503.

[8.] N. Krasteva, I. Besnard, B. Guse, R. E. Bauer, K. Mullen, A. Yasuda, T. Vossmeyer, *Nano Letters* **2002,** *2* 551-555.

[9.] H. Wohltjen, A. W. Snow, *Analytical Chemistry* **1998,** *70* 2856-2859.

[10.] F. P. Zamborini, M. C. Leopold, J. F. Hicks, P. J. Kulesza, M. A. Malik, R. W. Murray, *Journal of the American Chemical Society* **2002,** *124* 8958-8964.

[11.] M. F. Crommie, C. P. Lutz, D. M. Eigler, *Science* **1993,** *262* 218-220.

[12.] H. Ohnishi, Y. Kondo, K. Takayanagi, *Nature* **1998,** *395* 780-783.

[13.] R. P. Andres, J. D. Bielefeld, J. I. Henderson, D. B. Janes, V. R. Kolagunta, C. P. Kubiak, W. J. Mahoney, R. G. Osifchin, *Science* **1996,** *273* 1690-1693.

[14.] H. Imamura, J. Chiba, S. Mitani, K. Takanashi, S. Takahashi, S. Maekawa, H. Fujimori, *Physical Review B* **2000,** *61* 46-49.

[15.] A. A. Middleton, N. S. Wingreen, *Physical Review Letters* **1993,** *71* 3198-3201.

[16.] P. E. Trudeau, A. Escorcia, A. A. Dhirani, *Journal of Chemical Physics* **2003,** *119* 5267-5273.

[17.] T. Sato, H. Ahmed, D. Brown, B. F. G. Johnson, *Journal of Applied Physics* **1997,** *82* 696-701.

[18.] C. Thelander, M. H. Magnusson, K. Deppert, L. Samuelson, P. R. Poulsen, J. Nygard, J. Borggreen, *Applied Physics Letters* **2001,** *79* 2106-2108.

[19.] M. Brust, D. Bethell, D. J. Schiffrin, C. J. Kiely, *Advanced Materials* **1995,** *7* 795-&.

[20.] A. Rosidian, Y. J. Liu, R. O. Claus, *Advanced Materials* **1998,** *10* 1087-+.

[21.] E. Braun, Y. Eichen, U. Sivan, G. Ben-Yoseph, *Nature* **1998,** *391* 775-778.

[22.] J. D. Le, Y. Pinto, N. C. Seeman, K. Musier-Forsyth, T. A. Taton, R. A. Kiehl, *Nano Letters* **2004,** *4* 2343-2347.

[23.] Y. Maeda, H. Tabata, T. Kawai, *Applied Physics Letters* **2001,** *79* 1181-1183.

[24.] H. Y. Li, S. H. Park, J. H. Reif, T. H. LaBean, H. Yan, *Journal of the American Chemical Society* **2004,** *126* 418-419.

[25.] A. Kumar, M. Pattarkine, M. Bhadbhade, A. B. Mandale, K. N. Ganesh, S. S. Datar, C. V. Dharmadhikari, M. Sastry, *Advanced Materials* **2001,** *13* 341-344.

[26.] H. Nakao, H. Shiigi, Y. Yamamoto, S. Tokonami, T. Nagaoka, S. Sugiyama, T. Ohtani, *Nano Letters* **2003,** *3* 1391-1394.

[27.] M. G. Warner, J. E. Hutchison, *Nature Materials* **2003,** *2* 272-277.

[28.] G. Decher, *Science* **1997,** *277* 1232-1237.

[29.] W. Fischer, S. Markwitz, H. Labischinski, *European Journal of Biochemistry* **1997,** *244* 913-917.

[30.] R. J. Doyle, M. L. McDannel, J. R. Helman, U. N. Streips, *J Bacteriol* **1975,** *122* 152-8.

[31.] M. Virta, S. Lineri, P. Kankaanpaa, M. Karp, K. Peltonen, J. Nuutila, E. M. Lilius, *Appl.Environ.Microbiol.* **1998,** *64* 515-519.

[32.] E. Traversa, *Sensors and Actuators B-Chemical* **1995,** *23* 135-156.

[33.] S.O.Kasap, *Principals of Electrical Engineering materials and devices*, McGraw-Hill, New York **1997,** pp. 284-287.

Figure: 1: *Highly controlled, highly selective deposition of Au nanoparticle on bacteria:* Lysine coated 30 nm Au nanoparticle deposition from pH 7 solution for (a) 30 min, (b) 1 hr, (c) 2 hr, (d) 4hr, and (e) 8 hr. (f) Same (positively charged) Au nanoparticles are deposited on a (negatively charged) PSS coated lysine/SiO_2/Si substrate for 16 hrs. The Au nanoparticles are percolating after 4 hr. deposition on bacteria while no conduction is observed for the physical surface in (f). Bar size = 300 nm. The small amount of multi-layer formation for high deposition time is due to contraction of the membrane because of loss of water in Scanning Electron Microscope.

Figure 2: *Schematic of the closely packed nanoparticle:* Schematic showing two lysine coated Au nanoparticles clutched by negatively charged teichoic acid molecules. The distance between Au nanoparticle surfaces is a. The electron transport from right to left is through a mixture of organics (lysine, teichoic acid) and air. The role of the electric field inducing electron transport is discussed later in Figs. 4 and 5.

Figure 3: *The fate of the bacteria during device processing:* The standard PI/SYTO 9 assay is used to probe the survival of the bacteria at various stages of the process. Confocal microscopy of different samples at following stages is shown: (a) Bacteria immediately after immobilization from the nutrient broth on the substrate; (b) after the gold nanoparticle deposition for 4 hrs.; and (c) after 10^{-5} torrs vacuum for 2 hrs. The green and red coloration indicate that the bacteria are alive and dead, respectively.

Figure 4: *The characteristics of the humidity sensor:* Typical device current as a function of relative humidity for “up” (i.e., humidity decreasing) and “down” cycles. The current is normalized per bridge. The inset shows two typical bacteria

bridges spanning between the electrodes. The peripherals strip is a (percolating) monolayer deposition of nanoparticle.

Figure 5: *The validity of model and Peptidoglycan actuation:* (a) The comparison of theory (solid lines) in Eq. (1) and experimental observation (data points) are compared at various bias for the same device. The consecutive measurements on the device are made at increasing bias, i.e., 5, 10, 15, 20, and 25 V. The inset shows the four fitting parameters, K, f, T_0 and R_B. (b) Shows the corrected current (after subtracting the calculated leakage current, I_B) as a function of calculated percent change in inter-particle distance due to humidity induced dimensional change in the peptidoglycan membrane. Consistent with the model Eq. (1), the straight line for all biases in the semi-log plot indicates exponential dependence. The inset shows the (non-ohmic) I-V characteristics and differential conductance.

Figure 6: *Temperature dependence of the device current at 0% humidity:* Plot of negative of natural logarithm of current versus 100/T with applied bias of 0.1 V. The units for I, T and kT (for the formula in the in-set) are A, K and eV, respectively.

TOC - Figure

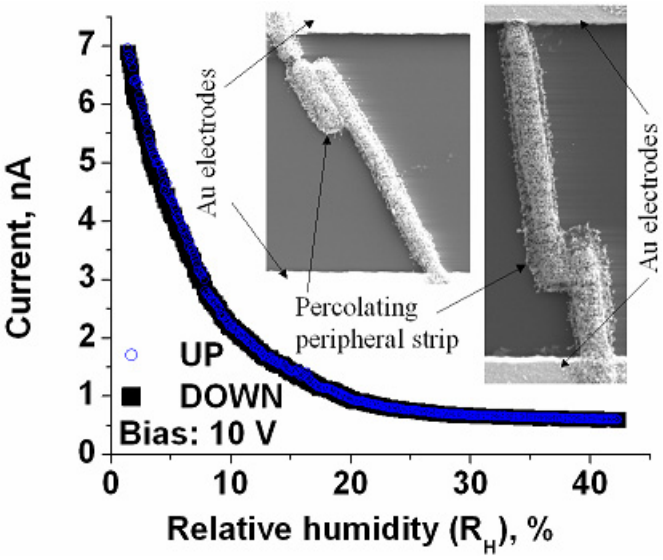

Bacteria-nanoparticle hybrid device is operated by applying a bias of 10V across the bacterial bridge and measuring the device current. Typical current as a function of relative humidity for "up" (i.e., humidity decreasing) and "down" cycles shows no hysteresis and a 40-fold change (after background subtraction). The inset shows two typical bacterial bridges spanning between the electrodes. The peripherals strip is a monolayer deposition of nanoparticles that leads to a constant background.

Keywords:
Bioelectronics, nanodevice, sensor, Au nanoparticle, nanoparticle monolayer, nanoparticle self-assembly

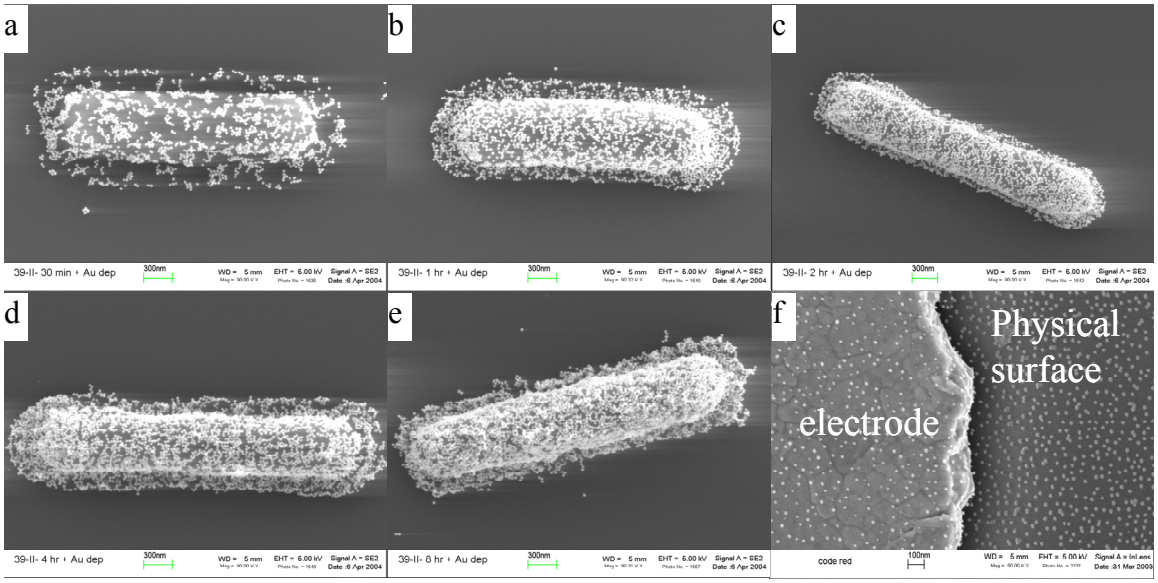

FIGURE 1:

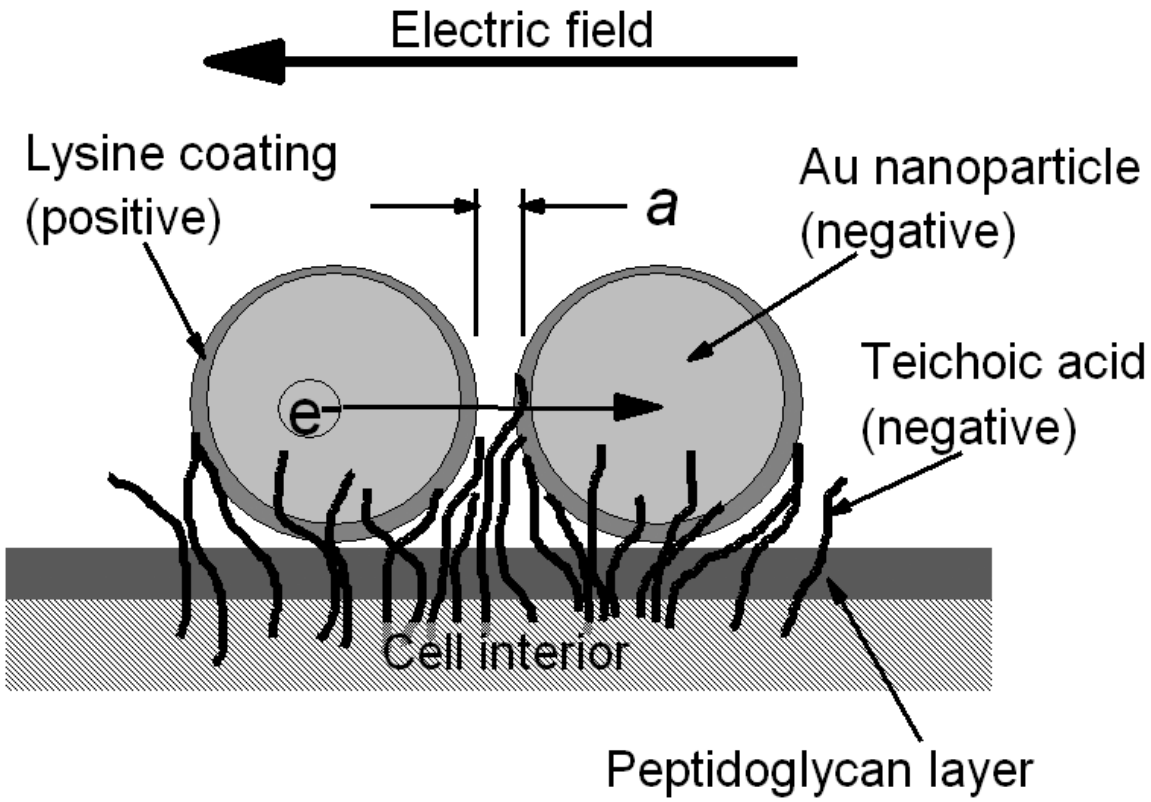

FIGURE 2

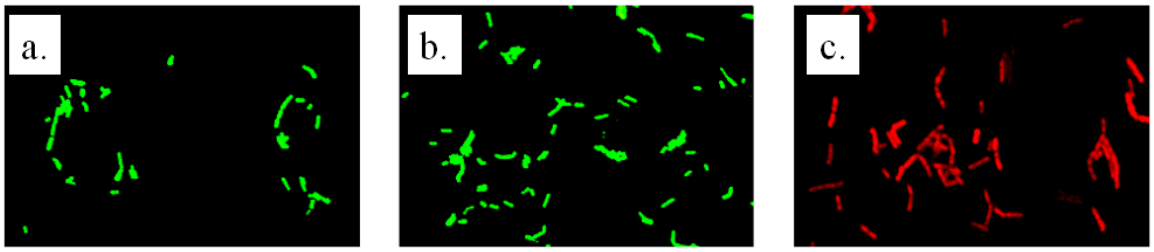

FIGURE 3:

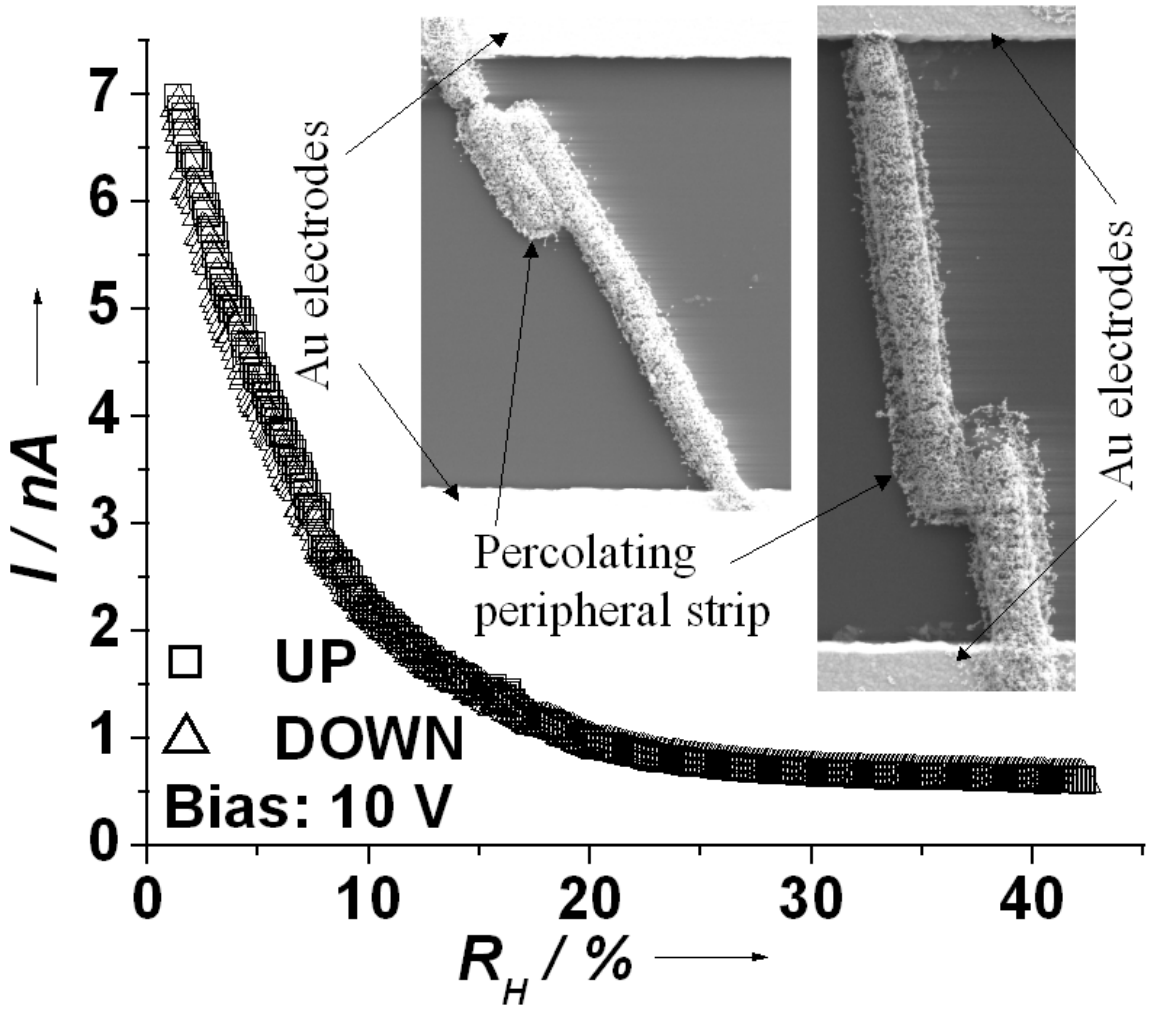
I / nA
R_H / %
UP
DOWN
Bias: 10 V
Au electrodes
Percolating
peripheral strip
Au electrodes

FIGURE 4:

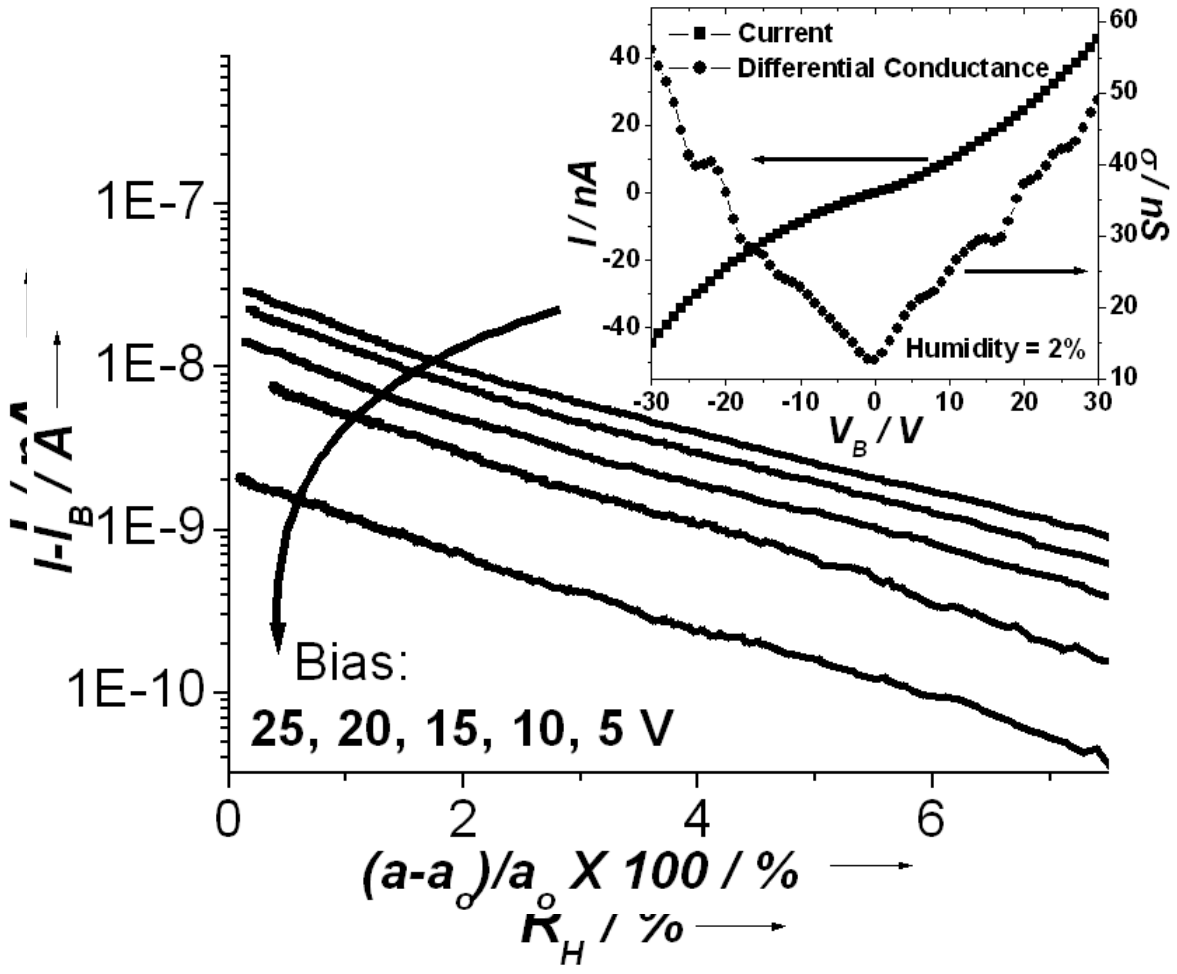

FIGURE 5 (a)

FIGURE 5 (b)

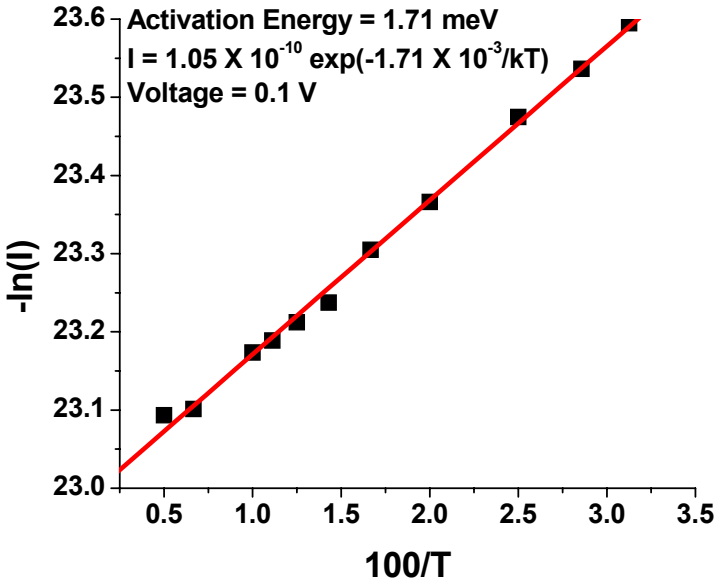
Activation Energy = 1.71 meV
I = 1.05 X 10^-10 exp(-1.71 X 10^-3/kT)
Voltage = 0.1 V
-ln(I)
100/T
23.6
23.5
23.4
23.3
23.2
23.1
23.0
0.5
1.0
1.5
2.0
2.5
3.0
3.5

FIGURE 6: